Research Square

Preprints are preliminary reports that have not undergone peer review.
They should not be considered conclusive, used to inform clinical practice,
or referenced by the media as validated information.

Sugarcane Water Requirement and Yield Projections in Major Producing Regions of China Under Future Climate Scenarios

Xiaochen ZHU (xiaochen.zhu@nuist.edu.cn)
Nanjing University of Information Science and Technology
Hengxin DONG
Nanjing University of Information Science and Technology
Qiangyu LI
Nanjing University of Information Science and Technology
Xinfa QIU
Nanjing University of Information Science and Technology
Yu Sun
Nanjing University of Information Science and Technology

Research Article

Keywords: water requirement of sugarcane, CLDAS, random forest, sugarcane yield, climate scenarios

Posted Date: May 9th, 2022

DOI: https://doi.org/10.21203/rs.3.rs-1627793/v1

License: This work is licensed under a Creative Commons Attribution 4.0 International License.
Read Full License

Sugarcane Water Requirement and Yield Projections in Major Producing Regions of China Under Future Climate Scenarios

Xiaochen ZHU[1,2*], Hengxin DONG[1], Qiangyu LI[1], Xinfa QIU[3], and Yu Sun[4]

Abstract

Relative soil moisture is of great significance to the growth and yield of sugarcane. In this study, we use the relative soil moisture from the China Meteorological Administration Land Data Assimilation System (CLDAS) to dynamically evaluate the water requirement of sugarcane and its growth adaptability at different growth stages. Based on the data of relative soil moisture, air temperature, precipitation and soil temperature, a sugarcane yield model is established to analyze the projected change trends of sugarcane yield in China from 2020 to 2100 under three future scenarios. Analysis results show that sugarcane requires more water during the elongation stage but less water at the ripening stage. The relative soil moisture from the CLDAS can be used to calculate the proportion of the daily suitable area to the total planting area. The combining of relative soil moisture data and water requirement indicators can better characterize the water requirement during sugarcane growth. Suitable relative soil moisture during the tillering and elongation stages is the most critical factor that directly affects the sugarcane yield. From 2020 to 2100, sugarcane yield will increase first and then decrease sharply. The increase in emissions can lead to an apparent downward trend in sugarcane yield. Based on the CLDAS data and water requirement indicators, a new method for monitoring the sugarcane growth throughout the growth period is proposed in this study. In the SSP370 and SSP460 scenarios, the sugarcane yield showed a downward trend, and there were mutations in 2064 and 2052, respectively. After the mutation, the yield decline trend was more obvious. Under the SSP585 scenario model, the sugarcane production showed an upward trend from 2022 to 2033, and a downward trend after 2033, and a mutation occurred in 2051. After the mutation,

the downward trend of sugarcane production was more obvious.

Key words: water requirement of sugarcane, CLDAS, random forest, sugarcane yield, climate scenarios

1. Introduction

Sugarcane is an important raw material for sugar production, and the bagasse can also be used to produce energy such as alcohol (Christofoletti et al. 2013; Jaiswal et al. 2017). China is the third-largest sugar-producing country after Brazil and India, where the sugar production reached 2.2319 million tons in 2019, which acts as an essential part of the agricultural trade (Zu et al. 2018). In China, sugarcane is mainly cultivated in Guangxi Zhuang Autonomous Region, Guangdong Province, Yunnan Province and Hainan Province. The gross product of the sugarcane sugar industry is 6.86 billion dollar, with the farmer income being 5.08 billion dollar, which is an essential source of income for farmers (Li and Yang 2015). Therefore, the forecasting of sugarcane yield and its change trend plays a vital role in the formulation of policies by relevant departments (Verma et al. 2021; Wang et al. 2017).

The China Meteorological Administration (CMA) Land Data Assimilation System (CLDAS) can provide a land surface dataset (available online at

Xiaochen Zhu
xiaochen.zhu@nuist.edu.cn
Hengxin Dong
hengxin_dong@163.com
Qiangyu Li
20201208014@nuist.edu.cn
Xinfa Qiu
xfqiu135@nuist.edu.cn
Yu Sun
yu_s.un@foxmail.com
1 School of Applied Meteorology, Nanjing University of Information Science and Technology, Nanjing, 210044
2 Jiangsu Key Laboratory of Agricultural Meteorology, Nanjing University of Information Science and Technology, Nanjing 210044
3 School of Geographical Sciences, Nanjing University of Information Science and Technology, Nanjing, 210044
4 School of Atmospheric Sciences, Nanjing University of Information Science and Technology, Nanjing, 210044

http://data.cma.cn/search/uSearch.html?keywords=CLDAS) with high spatio-temporal resolutions (Xie et al. 2017). Another datasets of the same type are the Global Land Data Assimilation System (GLDAS) dataset and North American Land Data Assimilation project (NLDAS), which are also widely used in agricultural land drought studies and crop yield studies: Fang(2021) studied the Soil Water Deficit Index (SWDI) and Soil Moisture Deficit Index (SMDI) in spring and summer out of Australia using Soil Moisture Active Passive (SMAP) soil moisture (SM), GLDAS long-term SM and soil attribute products; Mokhtari (2018) input GLDAS data set and leaf area index data as driving factors into the Soil Water Atmosphere Plant (SWAP) model to predict wheat yield, the experimental results show that the accuracy of SWAP model is improved after combining GLDAS dataset. Xia (2014) used the NLDAS dataset to calculate drought indices for each region of the U.S. and to reconstruct typical drought events in U.S. history. CLDAS, NLDAS and GLDAS are all data sets generated by terrestrial assimilation systems. The CLDAS dataset, NLDAS dataset, and GLDAS dataset cover China, North America, and the world, respectively. For the study of the Chinese region, the CLDAS dataset has higher accuracy than the GLDAS dataset (Han et al. 2020; Sun et al. 2020), and this paper will be based on the CLDAS data.

Sugarcane-related researches mainly focus on remote sensing-based planting area extraction and growth monitoring and yield prediction, among which the research on sugarcane planting area extraction is relatively mature at present (Aguiar et al. 2011; Wang et al. 2019). There are also related studies on sugarcane yield prediction, but most of these studies are based on satellite remote sensing supplemented by crop models to experiment with sugarcane yield prediction. Rampazo and Núria (2021) combined the Moderate-Resolution Imaging Spectroradiometer (MODIS) images and the Simple Algorithm for Retrieving Evapotranspiration model to analyze sugarcane growth situation in southern Brazil. However, timely monitoring of soil water deficits cannot be realized by MODIS because of its long production cycle (8 or 16 days). Based on Landsat images, Almeida (2006) studied the spectral characteristics of sugarcane at different growth stages to estimate sugarcane yield. However, satellites like Landsat are susceptible to cloud cover (Dong and Menzel 2016; Foga et al. 2017). With the rapid development of artificial intelligence technology in recent years, some scientists have successively introduced machine learning technology to sugarcane yield forecasting. (Fernandes et al. 2017) obtained the NDVI index through the MODIS sensor, and used the NDVI index combined with the ANN neural network to evaluate the sugarcane yield status. (Xu et al. 2020) used UAV-LIDAR data to simulate sugarcane yield in Chongzuo City, Guangxi Province based on the random forest algorithm. The results show that the random forest algorithm is more effective than the traditional linear regression, and the fitting accuracy is higher. Neither the analysis on sugarcane yield at LIDAR or stations nor the research on different growth stages of sugarcane by satellite remote sensing can meet the requirements of large scale, high spatio-temporal resolutions and strong interference resistance.

The CLDAS can overcome the influence of cloud cover on the monitoring of surface meteorological elements (Chen and Yuan 2020), which has good adaptability to soil moisture monitoring (Long et al. 2019). The dataset has the advantage of short update period and high accuracy for short-term weather condition monitoring, and has achieved well research results in soil moisture monitoring (Suon et al. 2019; Wang and Yu 2021; Yu et al. 2019) and regionalization of crop growth adaptability (Rongsheng et al. 2020; Rongsheng et al. 2021).

The purpose of this study is to set the adaptable indicators for soil water requirement at different sugarcane growth stages according to the relative soil moisture, realize daily growth dynamic monitoring based on high-resolution data from CLDAS, and use CMIP6-related data combined with random forest algorithm to determine sugarcane yield under different scenarios and analyze the trend of the future sugarcane yield.

2. Data and methods

2.1 Study area and data description

2.1.1 Data description

The data used in this study include the basic geographic information data, CLDAS version 2.0 data, information from statistical yearbooks and outputs of the Coupled Model Intercomparison Project Phase 6 (CMIP6) models under future scenarios. Specifically, the basic geographic information data include three administrative boundaries at provincial, municipal and county levels and 1-km digital elevation model data.

CLDASV2.0 data coverage is 0-65°N, 60-160°E, with extremely high spatial and temporal resolution (spatial resolution 0.0625°, time resolution 1 hour, start in 2017). The product includes atmospheric driving field products (2m air temperature, 2m specific humidity, 10m wind speed, surface pressure, precipitation, shortwave radiation), surface temperature analysis products, soil moisture products (vertically divided into 5 layers: 0-5, 0 -10, 10-40, 40-100, 100-200cm), soil temperature analysis products (vertically divided into 5 layers: 5, 10, 40, 100, 200cm) and soil relative humidity analysis products (vertically divided into 3 layers: 0-10cm, 0-20cm, 0-50cm). The dataset is developed by combining satellite observation data and soil observation data, and is developed using techniques such as multi-grid variational assimilation, optimal interpolation, probability density function matching, physical inversion, and terrain correction. It has extremely high accuracy in China. Based on the integration of multiple land surface models, the CLDAS version 2.0 dataset used in this study include relative soil moisture, maximum temperature, average temperature, average wind speed, soil temperature and precipitation.

Through provincial and municipal statistical yearbooks, the sugarcane yields in main producing regions of China from 2017 to 2019 are obtained at provincial, municipal and county levels. Considering the regional applicability of the model (Zhu et al. 2020), the data selected for yield model construction and prediction include the soil moisture and maximum field capacity from the Canadian Earth System Model version 5 (CanESM5) (Sospedra-Alfonso et al. 2021) of CMIP6 during 2020–2100, the soil temperature and air temperature from the low resolution of climate model 6A of Institut Pierre-Simon Laplace (IPSL-CM6A-LR) model (Boucher et al. 2020), and the precipitation flux and 10-m wind speed from the version 2.1 of Goddard Institute for Space Studies (GISS-E2.1-G) model (Kelley et al. 2020; Nazarenko et al. 2022).

Each model contains multiple shared socio-economic pathways (SSPs) (Popp et al. 2017), from which we select three scenario models: SSP370, SSP460, and SSP585. The SSP370 scenario represents the medium to high end of the range of future forcing pathways, the radiative forcing is 7.0 W/m^2 and the temperature increase is about 2.8°C by 2100 (Zhao et al. 2020). The SSP460 scenario represents the medium range of future forcing pathways, the radiative forcing is 6.0 W/m^2 and the temperature increase is about 1.8°C by 2100 (Pu et al. 2020). The SSP585 scenario represents the high range of future forcing pathways, the radiative forcing is 8.5 W/m2 and the temperature increase is about 3.2°C by 2100 (O Neill et al. 2017; O'Neill et al. 2016). All data are interpolated to 0.0625°, and data available online at: https://esgfnode.llnl.gov/projects/cmip6/.

2.1.2 Study area

The study area covers four provinces, namely Guangxi Zhuang Autonomous Region, Guangdong Province, Yunnan Province and Hainan Province, where the annual yield of sugarcane accounts for more than 90% of the total sugarcane yield in China. The elevation distribution map (Fig. 1) shows that the western part of the study area is relatively high, and the terrain gradually tends to flatten out from the west to the east. The western part is Yunnan Province, located to the southeast of the Hengduan Mountains, which is an essential part of the Yunnan-Guizhou Plateau. The central part is Guangxi Zhuang Autonomous Region, which is mostly hilly. The eastern part is Guangdong Province, located in the Pearl River Delta region, with numerous alluvial plains. While the southern part is Hainan Province, whose terrain is low around and high in the middle. It can be seen that the major sugarcane producing areas in China belong to the subtropical monsoon climate zone, where the rainy and high-temperature seasons coincide, with the annual sunshine hours being 1000–3000 hours and the annual precipitation being 900–2600 mm (Guga et al. 2021).

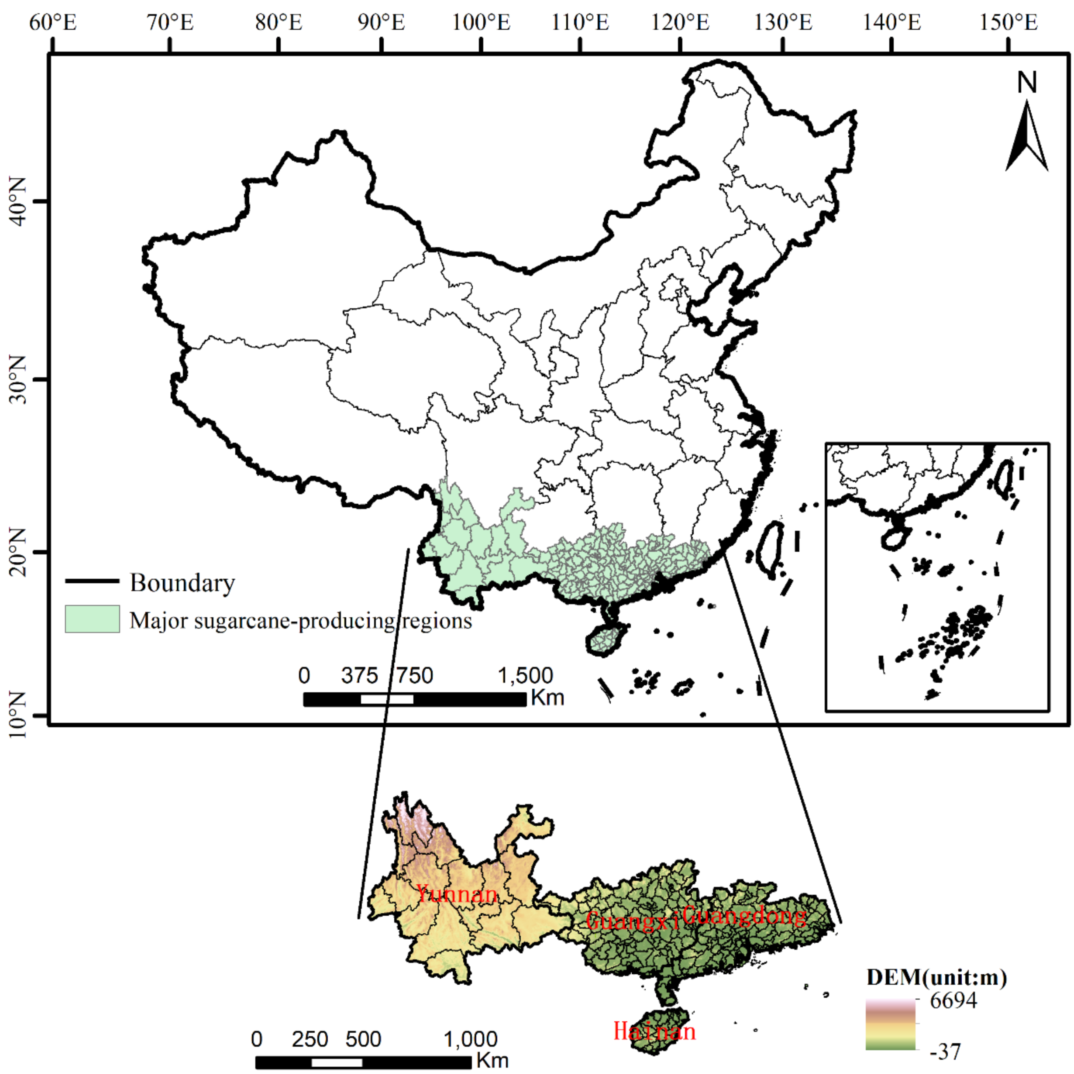

FIG. 1. The elevation distribution of major sugarcane producing regions in China.

2.2 Methods

2.2.1 Sugarcane water requirement

Water requirement during the crop growth period is one of the critical factors that determine the crop yield, and thus a reasonable evaluation of the soil moisture content throughout the growth period plays a vital role in estimating sugarcane yield. Based on previous studies on sugarcane water requirements (Guozhang 1993; Zhaomin 2019), this study summarizes the previous studies on water requirements of sugarcane to classify the sugarcane growth adaptability. The values of relative soil moisture corresponding to different sugarcane growth stages are shown in Table 1, which can be divided into three grades of most adaptable, adaptableand unadaptable. The sugarcane growth period is divided into four stages, namely germination-seedling, tillering, elongation and ripening stages. The soil depth suitable for sugarcane growth varies at different growth stages, which is relatively shallow in the germination-seedling stage and relatively deep in the middle and late stages due to the more extended root system.

TABLE 1. Adaptable indicators for soil water requirement at different sugarcane growth stages.

Indicators	Relative soil moisture (%)			
	Germination-seedling stage (20-cm soil layer)	Tillering stage (50-cm soil layer)	Elongation stage (50-cm soil layer)	Ripening stage (50-cm soil layer)
Most adaptable	$65 \leqslant R_{SM} < 75$	$70 \leqslant R_{SM} < 80$	$75 \leqslant R_{SM} \leqslant 90$	$50 \leqslant R_{SM} \leqslant 60$
Adaptable	$75 \leq R_{SM} < 85$ $55 \leqslant R_{SM} < 65$	$80 \leq R_{SM} < 90$ $60 \leqslant R_{SM} < 70$	$90 \leq R_{SM} < 95$ $65 \leqslant R_{SM} < 75$	$60 \leq R_{SM} < 70$ $40 \leqslant R_{SM} < 50$
Unadaptable	$R_{SM} \geq 85$ $R_{SM} < 55$	$R_{SM} \geq 90$ $R_{SM} < 60$	$R_{SM} \geq 95$ $R_{SM} < 65$	$R_{SM} \geq 70$ $R_{SM} < 40$

The periods and days corresponding to different growth stages are shown in Table 2. The entire growth period of sugarcane lasts 313 days, with 79 days for the germination-seedling stage, 21 days for the tillering stage, 182 days for the elongation stage (the longest) and 31 days for the ripening stage (Zhaomin 2019). Note that the growth periods and days are obtained based on the regional average, while the actural growth periods and days vary due to different producing regions, years and sugarcane varieties.

TABLE 2. Growth periods and days of sugarcane at different growth stages.

Growth stages	Periods	Days (d)
Germination-seedling stage	02.21-05.10	79
Tillering stage	05.11-05.31	21
Elongation stage	06.01-11.30	182
Ripening stage	12.01-12.31	31
Entire growth period	02.21-12.31	313

2.2.2 Sugarcane yield model construction

In addition to relative soil moisture, the growth of sugarcane is also closely related to meteorological conditions. Air temperature and relative soil moisture are important factors affecting the growth and development of sugarcane, and relative soil moisture is also affected by wind speed, soil temperature and precipitation (Saeed et al. 2022). Random forest algorithm (Breiman 2001) is a popular machine learning algorithm that can be used to solve classification problems and regression problems. Compared with other machine learning methods, it does not need to consider parameter covariance, does not need to do variable selection, has a high tolerance in outliers and noise, and is not prone to overfitting, has the advantages of good stability and high prediction accuracy (Yuan and Hu 2021). Its main idea is to draw n samples from the original training set with release, and the sample size of each sample is the same as the size of the original training set; then each sample is modeled as a decision tree separately, and n modeling results are obtained, and finally the average of each decision tree prediction result is used as the final prediction result (Rajković et al. 2022).

Based on the random forest algorithm, the relative soil moisture data, air temperature data, soil temperature data, precipitation data, and wind speed data in the CLDAS dataset were used to train the random forest model by using the sugarcane yield in each region from 2017 to 2019. The relative soil moisture data, air temperature data, soil temperature data, precipitation data, and wind speed data from CMIP6 were then input into the random forest model to forecast sugarcane yields for 2020-2100 under different scenarios. A total of 277 areas with sugarcane yields have been collected in this study, of which 10% of the yield data are used for verification, while the rest are adopted as training samples. The constructed sugarcane yield model is as follows (Eq. 1).

$$\mathrm{Yield}_{i,j} = f\left(\mathrm{GST}_{i,j}, \mathrm{PRE}_{i,j}, \mathrm{RSM}_{i,j}, \mathrm{TMP}_{i,j}, \mathrm{TMP\_MAX}_{i,j}, \mathrm{WIN}_{i,j}, a\right) \tag{1}$$

where $\mathrm{Yield}_{i,j}$ represents the sugarcane yield on the grid (i,j), $\mathrm{GST}_{i,j}$ the soil temperature, $\mathrm{PRE}_{i,j}$ the precipitation, $\mathrm{RSM}_{i,j}$ the relative soil moisture, $\mathrm{TMP}_{i,j}$ the daily average temperature, $\mathrm{TMP\_MAX}_{i,j}$ the maximum daily average temperature, $\mathrm{WIN}_{i,j}$ the 10-m wind speed, and a the empirical coefficient. i and j refer to the row and column numbers of raster data, respectively.

According to the above random forest model construction process, Fig 2 shows the flow chart of random forest model construction, code available online at: https://github.com/FunnyBiscuit613/random-forest.git.

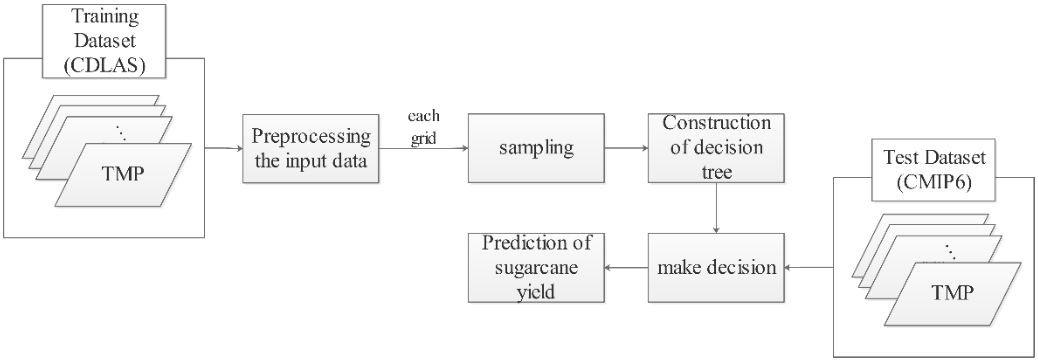

FIG. 2. Flow chart of sugarcane yield prediction based on random forest algorithm.

2.2.3 Data quality verification

In this study, three indicators of absolute error (Gao 2021), relative error (Mohammadi et al. 2015) and root-mean-square error (Wessel et al. 2018) are adopted to perform quality verification analysis. The absolute error measures the difference between the fitted and actual values, whose expression is given below (Eq. 2).

$$\mathrm{MAE} = \frac{\sum_{i=1,j=1}^{m,n} \left(x_{i,j} - y_{i,j}\right)^2}{m \times n} \tag{2}$$

where MAE indicates the absolute error; $x_{i,j}$ the fitted sugarcane yield from pixel to pixel under different scenarios; $y_{i,j}$ the pixel-by-pixel value of the actual yield data; i and j the row and column of the current pixel; m and n denote the maximum numbers of rows and columns.

The mean relative errors (MRE) measures the confidence level of the fitted value, which can be expressed as follows (Eq. 3).

$$\mathrm{MRE} = \frac{\sum_{i=1,j=1}^{m,n} \frac{x_{i,j} - y_{i,j}}{y_{i,j}}}{m \times n} \times 100\% \tag{3}$$

The root-mean-square error (RMSE) is adopted to measure the deviation between fitted value and actual value, and it can be expressed as follows (Eq. 4).

$$\mathrm{RMSE}=\sqrt{\frac{\sum_{i=1,j=1}^{m,n}\left(x_{i,j}-y_{i,j}\right)^2}{m\times n}} \tag{4}$$

2.2.4 Mann-Kendall test

The Mann-Kendall test has been widely applied in the analysis of abrupt climate changes in fields including meteorology, climatology, hydrology (Gocic and Trajkovic 2013; Wang 2020). In this study, the Mann-Kendall test is applied to analyze the abrupt changes in the long-term time series of sugarcane yield based on the simulations from 2020 to 2100. The most distinguishing feature of this method during a non-parametric test is that the test samples do not have to follow a specific distribution, and this method is independent of a few outliers. The UFK curve greater than 0 indicates an upward trend for the time series, while the curve less than 0 indicates a downward trend. When the curve exceeds the threshold (α=0.05), it indicates that the upward or downward trend is significant, and the part that exceeds α is the time range for abrupt change. UFK is a standard normal distribution, which is a series of statistics calculated in the order of time series x, UBK=-UFK. The intersection point between UFK and UBK curves is the abrupt change time (Wei 2007). In addition, the separate MK trend analysis does not take into account the seasonal cycle changes, and cannot take into account the impact of the previous time period on the current time period. Therefore, the Correlated Seasonal MK Test is carried out on the basis of the MK trend analysis to compare whether the results of the MK trend analysis and the Correlated Seasonal MK Test are consistent (Yue and Wang 2004; Yue and Wang 2002).

2.2.5 Technical process

In this study, the relative soil moisture data in the CLDAS dataset were used to delineate the different adaptability of sugarcane in conjunction with the optimum relative soil moisture indicators for sugarcane at different fertility stages in Table 1. Then the temperature data, precipitation data, wind speed data, soil temperature data in the CLDAS dataset, and actual sugarcane yield were used as the x and y variables in the model training. Finally temperature data, wind speed data, relative soil moisture data, and soil temperature data from CMIP6 were used as x variables in the test set to predict future sugarcane yields under different scenarios.

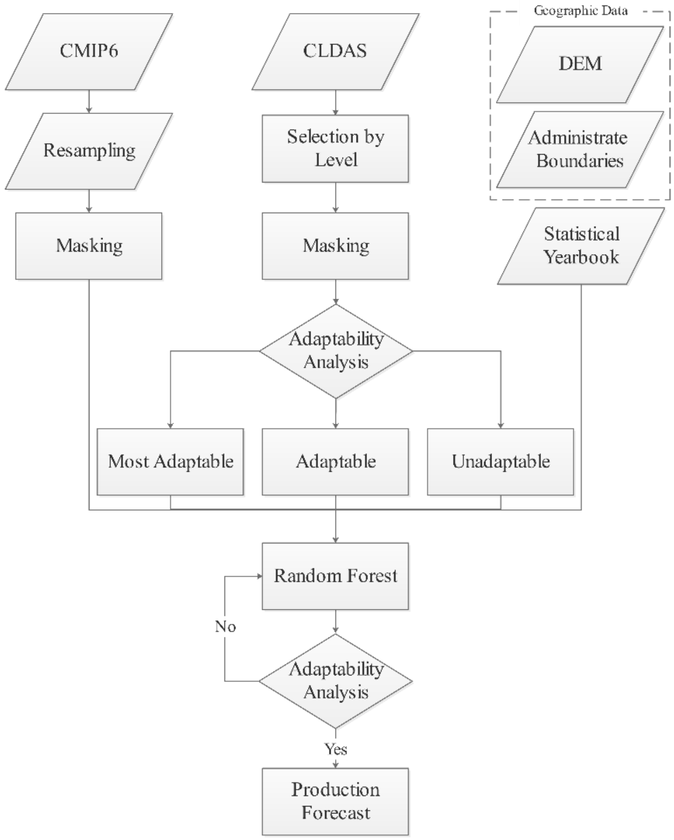

FIG. 3. Flow chart of sugarcane yield prediction based on random forest algorithm.

3. Results

3.1 Spatial distributions of soil moisture based on the CLDAS data

Requirements of soil water vary at different sugarcane growth stages, i.e., more water at the elongation stage and less water at the ripening stage. Based on the CLDAS data, the daily relative soil moisture at different soil depths that vary at different growth stages are obtained, of which the spatial distributions are shown in Fig. 4. Figure 4a shows the spatial distribution of relative soil moisture on April 1, 2019, when the sugarcane is at the germination-seedling stage. The result indicates that the relative soil moisture is relatively low in the Hengduan Mountains in northwestern Yunnan Province, which is not conducive to sugarcane growth. It is between 60% and 80% in the eastern part of Yunnan Province bordering Guangxi, which is suitable for sugarcane growth. In east Guangxi and Guangdong, the relative soil moisture is generally high (above 80%), which is prone to cause root rot of sugarcane seedlings, thus leading to yield reduction.

Generally, the relative soil moisture gradually increases from the west to the east. The spatial distribution on May 20, 2019 during the sugarcane tillering stage (Fig. 4b) shows that the relative soil moisture is relatively low in Yunnan, unfavorable to sugarcane growth. Guangxi and southern Guangdong have relative soil moisture of 60%–90%, which is adaptable for sugarcane growth. Guangdong Province has low relative soil moisture that is not conducive to sugarcane growth. In general, the relative soil moisture is low in the west and high in the east at the tillering stage. The spatial distribution of relative soil moisture on July 1, 2019 during the elongation stage (Fig. 4c) demonstrates that the soil moisture is relatively high in the southeast of Guangxi and the southern and northern regions of Guangdong. In northwestern Yunnan, the relative soil moisture is relatively low. While the junction of Yunnan and Guangxi as well as the northeastern part of Guangxi have relative soil moisture of 60%–90%, which is adaptable for sugarcane growth. Figure 4d illustrates the spatial distribution of relative soil moisture on December 1, 2019 during the ripening stage.

The result shows that the relative soil moisture in Hainan Province is relatively high, which is not conducive to sugar accumulation; while in eastern Yunnan, central Guangxi and southern Guangdong, the relative soil moisture is between 40% and 60%, adaptable for sugar accumulation.

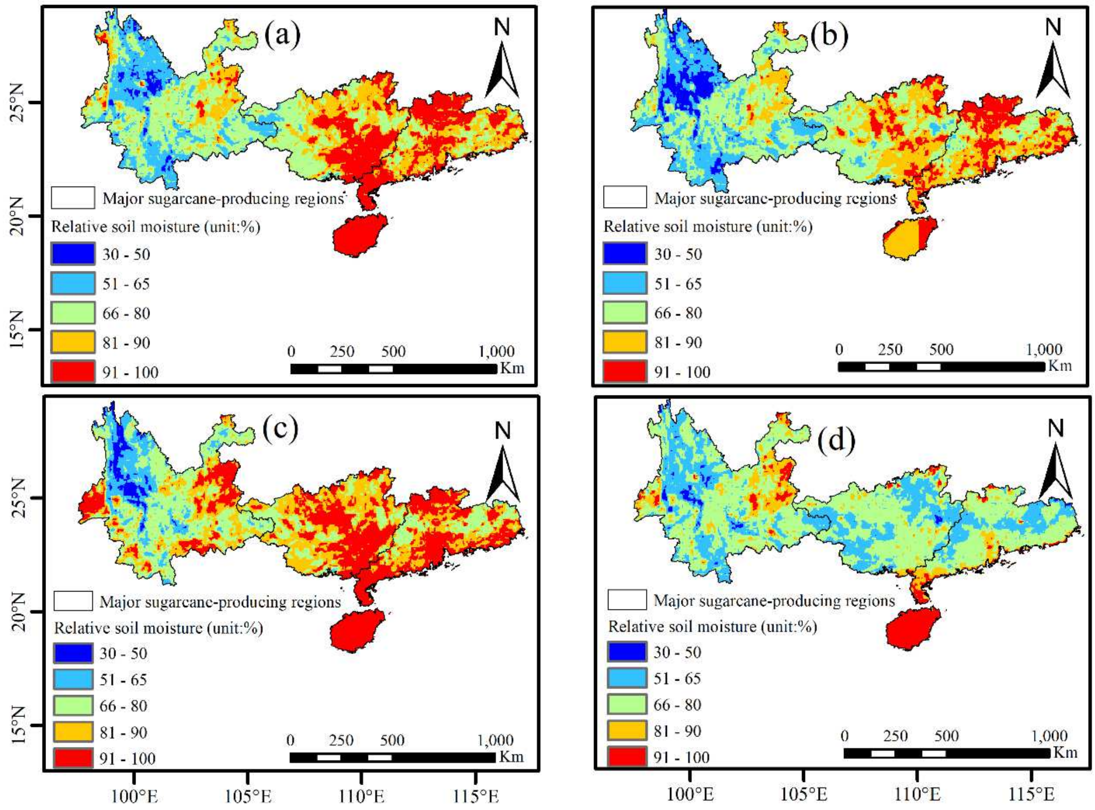

FIG. 4. Spatial distributions of relative soil moisture in the main sugarcane producing regions on (a) April 1, 2019 during the seedling-germination stage, (b) May 20, 2019 during the tillering stage, (c) July 1, 2019 during the elongation stage and (d) December 1, 2019 during the ripening stage.

3.2 Adaptability for sugarcane growth based on the CLDAS data

Based on the relative soil moisture from the CLDAS version 2.0 data and by referrring to the adaptable indicators of soil water requirement at different sugarcane growth stages (Table 1), the sugarcane growth adaptabilities on the above four representative dates are obtained, of which the spatial distributions are shown in Fig. 5.

Figure 5a shows the distribution of sugarcane growth adaptability on April 1, 2019. Since the sugarcane water requirement is not high at the germination-seedling stage, eastern Guangxi and Guangdong with high soil moisture are unadaptable for sugarcane growth, and even more, excessive soil moisture can inhibit sugarcane growth. Figure 5b presents the spatial distribution of sugarcane growth adaptability on May 20, 2019. Since the sugarcane water requirement gradually increases at the tillering stage, the regions with low relative soil moisture are no longer adaptable for sugarcane growth, and the unsuitable areas are mainly located in the Hengduan Mountains of western Yunnan and northern Guangdong. Figure 5c is the same as Fig. 5b, but for July 1, 2019 at the elongation stage, which is a critical stage for sugarcane growth, and the water requirement reaches the highest at this stage. Excessively low relative soil moisture can inhibit sugarcane growth. Therefore, the unsuitable regions are mainly concentrated in west Yunnan and southeast Guangxi. Figure 5d shows the sugarcane growth adaptability on December 1, 2019 at the ripening stage. Sugarcane water requirement is not high at this stage, and excessively high relative soil moisture can cause sugarcane re-growth or root rot, leading to a decrease in sugarcane yield. Therefore, northeastern Yunnan, central Guangxi, a few parts of southern and northern Guangdong, and Hainan are not adaptable for sugarcane growth.

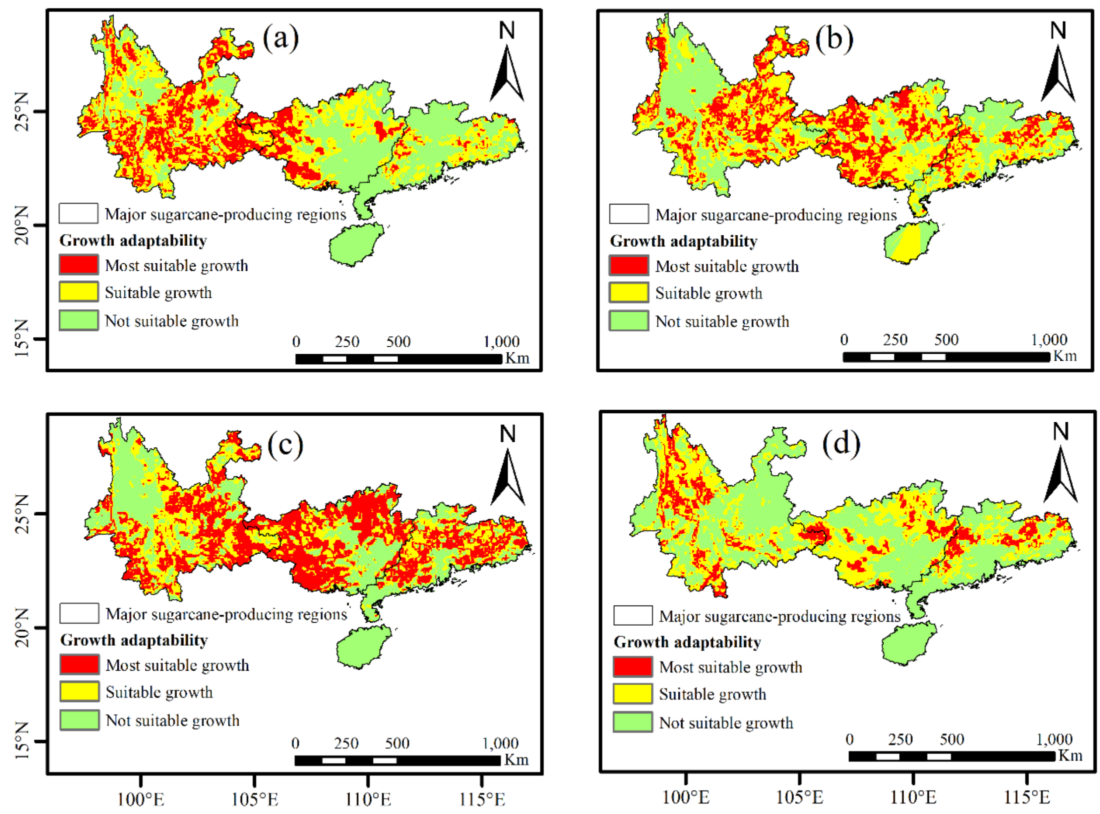

FIG. 5. Spatial distributions of adaptability in the main sugarcane producing regions on (a) April 1, 2019 during the seedling-germination stage, (b) May 20, 2019 during the tillering stage, (c) July 1, 2019 during the elongation stage and (d) December 1, 2019 during the ripening stage. (Based on the adaptability indicators in TABLE 1 and the relative soil moisture in FIG 4.)

3.3 Analysis of relative soil moisture in typical regions

In the main sugarcane producing areas of China, four typical regions of Fusui, Lincang, Xingbin and Danzhou are selected to analyze the changes of relative soil moisture over time and the corresponding sugarcane growth adaptability (Fig. 6).

As shown in Fig. 6a, the relative soil moisture can meet sugarcane growth needs at the germination-seedling stage in Fusui, and it is generally adaptable for sugarcane growth at the tillering and elongation stages. While at the ripening stage, the relative soil moisture is relatively high in Fusui, which is not conducive to sugar accumulation. Overall, the relative soil moisture in Fusui County basically meets sugarcane water requirement during the entire growth period. The sugarcane yield per unit area in Fusui was relatively high in 2019, reaching 87.1 $t \cdot ha^{-1}$.

In Lincang (Fig. 6b), the relative soil moisture generally meets the optimum demand of sugarcane growth at the seedling-germination stage. It is relatively low at the early and late elongation stage, while high at the ripening stage, which is not conducive to sugar accumulation. The sugarcane yield per unit area in Lincang was 63.2 $t \cdot ha^{-1}$ in 2019, basically the same as that in 2018 (63.0 $t \cdot ha^{-1}$).

In Danzhou (Fig. 6c), the relative soil moisture is abnormally high at the germination-seedling stage. It does not meet the optimum sugarcane growth conditions in the tillering stage except a few days. At the elongation stage, the relative soil moisture fluctuates at the upper limit of the optimum relative soil moisture, mostly higher than the optimum. Abnormally high relative soil moisture at the ripening stage can easily lead to sugarcane root rotting and death, thereby reducing the yield of sugarcane. In 2019, the relative soil moisture in Danzhou did not meet the water requirement of sugarcane growth, resulting in the sugarcane yield per unit area being only 55.8 $t \cdot ha^{-1}$.

For Xingbin (Fig. 6d), the relative soil moisture is abnormally high at the germination-seedling stage, which can easily cause seedling death and leading to yield reduction. At the early elongation stage, the relative soil moisture is greater than the optimum soil moisture; while in the middle and late stages, however, the relative soil moisture is adaptable for sugarcane growth. Losses caused by unexpected deaths at the sugarcane seedling stage can be saved by measures such as timely replanting. Therefore, although the relative soil moisture at the early stage failed to meet the optimum water requirement of sugarcane in Xingbin in 2019, the sugarcane yield per unit area still reached as high as 97.2 t·ha^{-1}.

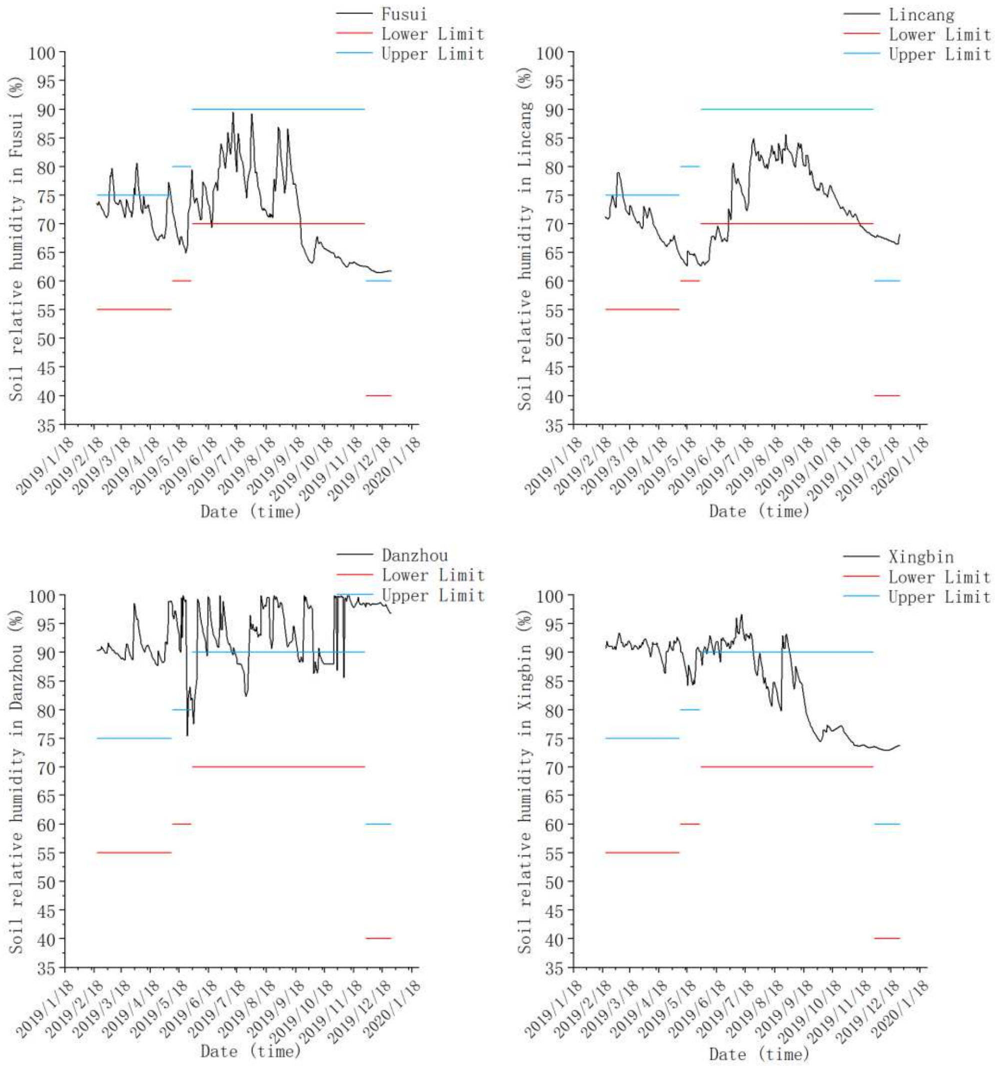

FIG. 6. Comparison of relative soil moisture and water requirement during the sugarcane growth period in 2019 in four typical regions of (a) Fusui, (b) Lincang, (c) Danzhou and (d) Xingbin.

3.4 Validation of sugarcane yield model and importance analysis of factors

As mentioned in section 2.2.2, 10% of the sample data are left to verify the performance of sugarcane yield model. Based on the three evaluation indicators, the quality evaluation results of the fitting yields are shown in Table 3. It can be seen that the RMSE and MRE of the fitted sugarcane yields under the SSP370 scenario are smaller than those under the other two scenarios, while the MAE of the yield is smaller under the SSP585 scenario than those under the other two scenarios. The overall performance reaches the best under the SSP370 scenario.

TABLE 3. Verifications of sugarcane yields simulated under different scenarios.

Year	SSP370			SSP460			SSP585		
	MAE	MRE	RMSE	MAE	MRE	RMSE	MAE	MRE	RMSE
2018	7.49	0.24	19.3	11.3	0.3	26.45	8.4	0.26	20.64
2019	2.09	0.024	15.09	10.5	0.12	24.46	0.7	0.007	14.63

The comprehensive error of the SSP370 scenario mode is the smallest, so taking the scenario as an example, the spatial distributions of relative errors for sugarcane yields in main sugarcane producing regions in China are shown in Fig. 7. Results show that the relative errors of sugarcane yields are greater than 100% in Kunming and Qujing of Yunnan, Liunan of Guangxi, Shantou of Guangdong and Lingshui of Hainan. The absolute values of relative errors are larger than 50% in southeastern Yunnan, northwestern and eastern Guangxi, central Guangdong and southeastern Hainan. In major sugarcane producing regions such as Xingbin, Fusui, Jiangzhou and Ningming, the absolute values of relative errors are smaller than 25%. In general, relative errors are relatively larger in the Yunnan-Guizhou Plateau, while relatively smaller in Guangxi and the plains of Guangdong.

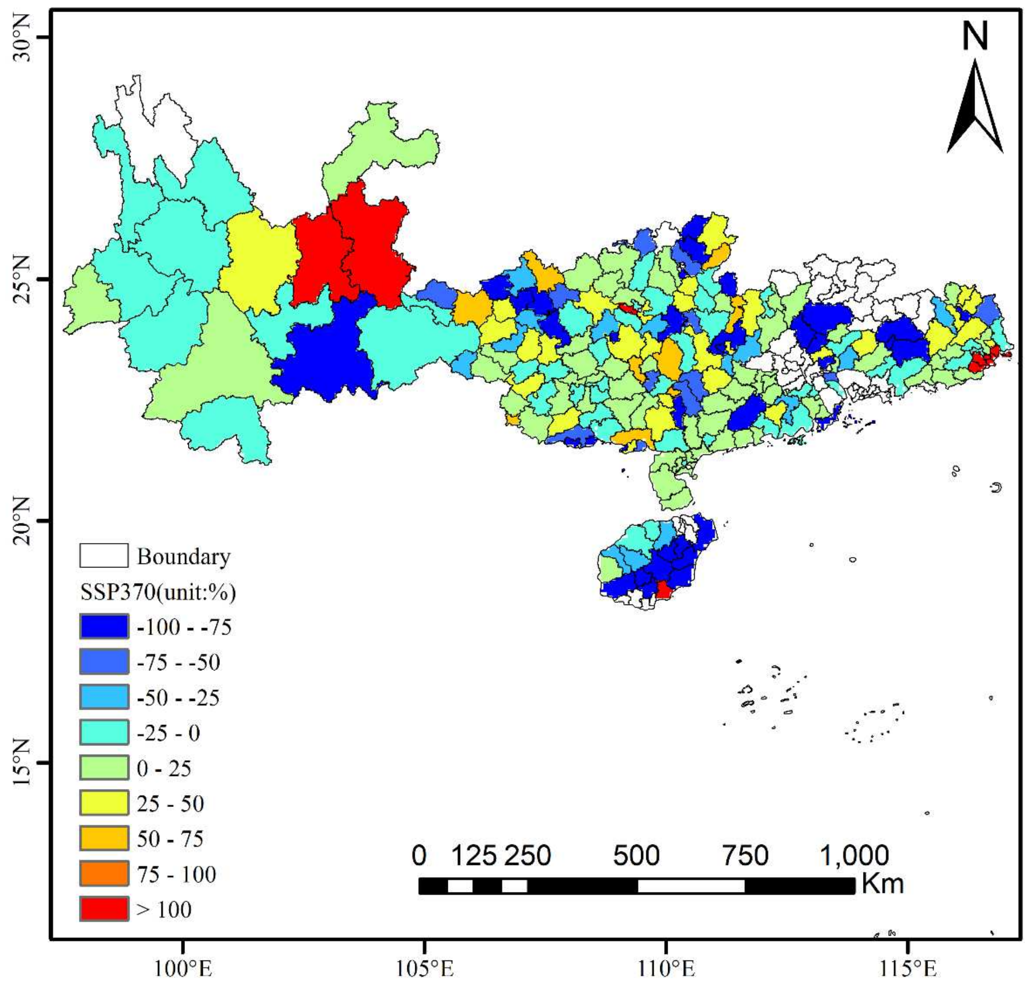

FIG. 7. Relative errors of sugarcane yields under the SSP370 scenario. The relative errors between simulated and actual sugarcane yields of CMIP6 for different years was calculated according to Eq 3.

Table 4 is a comparison table of the correlation coefficient and slope between different meteorological elements and sugarcane yield. From the analysis in Table 4, it can be seen that the relative soil moisture maintains a high correlation with sugarcane yield both in the correlation coefficient and the slope. Precipitation has the largest negative contribution to sugarcane yield among all variables

TABLE 4. Correlation coefficient and slope comparison table between different meteorological elements and sugarcane yield.

Variable	RSM	TMP	TMP-MAX	WIN	GST	PRE
Reg	0.165	-0.101	-0.044	0.067	-0.123	-0.143
R	0.165	-0.106	-0.048	0.068	-0.129	-0.156

3.5 Projected sugarcane yields under future scenarios

Figure 8 shows the results from the Mann-Kendall test for sugarcane yields under different scenarios. Under the SSP370 scenario (Fig. 8a), the UFK curve is firstly in the positive-value zone, indicating an upward trend of sugarcane yield. Then, the UFK curve is in the negative-value zone, suggesting that the sugarcane yield has a downward trend. From 2020 to 2100, the sugarcane yield shows a trend of first increasing and then decreasing, where an abrupt change appears in 2064. Figure 8b shows that the UFK curve is all in the negative-value zone under the SSP460 scenario, indicating that sugarcane yield has been in a decreasing trend, where an abrupt change appears in 2052. Under the SSP585 scenario (Fig. 8c), the change trend of sugarcane yield is generally similar to that under the SSP370 scenario, while the sudden change appears earlier in 2051, showing that the emission increase under the climate scenario makes the abrupt change appear earlier.

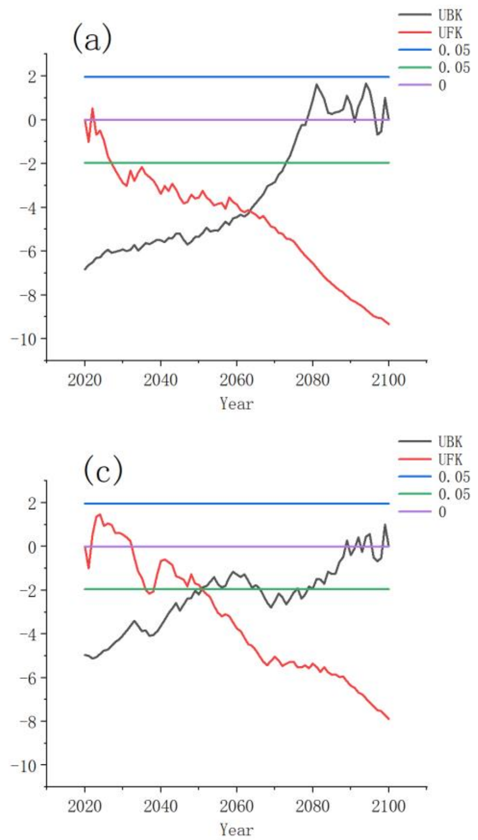

FIG. 8. Results of the Mann-Kendall test under different scenarios of (a) SSP370, (b) SSP460 and (c) SSP585.

The results of the Correlated Seasonal MK Test are shown in Table 5. According to the results of the Correlated Seasonal MK Test, the sugarcane yield showed a downward trend under the three scenarios of SSP370, SSP460 and SSP585, and they all passed the 0.05 significance test. The results of both trend tests indicated that the sugarcane yield would show a downward trend in the future. (P: p-value of the significance test; Z: normalized test statistics; Tau: Kendall Tau; S: Mann-Kendal's score; var_s: Variance S; slope: Theil-Sen estimator/slope; intercept: intercept of Kendall-Theil Robust Line, where full period cycle consider as unit time step)

TABLE 5 Correlated Seasonal MK Test results in different scenarios.

	P	Z	Tau	S	var_s	slope	intercept	trend
SSP370	0.01	-2.60	-0.72	-181.00	4847.67	-2.85	91.80	Decreasing
SSP460	0.02	-2.37	-0.55	-138.00	3388.67	-1.14	87.03	Decreasing
SSP585	0.01	-2.72	-0.79	-199.00	5361.00	-2.96	85.36	Decreasing

In this study, sugarcane yields in 2020, 2060 and 2100 under the low- and medium-emission scenario (SSP370) are selected to analyze their spatial variations in these three years. The sugarcane yield distributions in main producing regions under the SSP370 scenario are shown in Fig. 9. In 2020 (Fig. 9a), the regions with annual yield of sugarcane exceeding four million tons are concentrated in Lincang of Yunnan, Leizhou and Suixi of Guangdong, as well as Fusui and Xingbin of Guangxi. Compared with 2020, the sugarcane yield in 2060 (Fig. 9b) decreases by 0 to 578,000 tons. Among them, the sugarcane yield in Xingbin decreases the most. Figure 9c shows that the sugarcane yield in 2100 further decreases compared with that in 2060. Compared with 2020, the sugarcane yield in 2100 decreases by 0–1.39 million tons, where the yield decreases by 1.387 million tons in Xingbin and 1.3 million tons in Fusui. Overall, the sugarcane yield in 2100 drops by 18% approximately compared with that in 2020 in the main sugarcane producing regions of China.

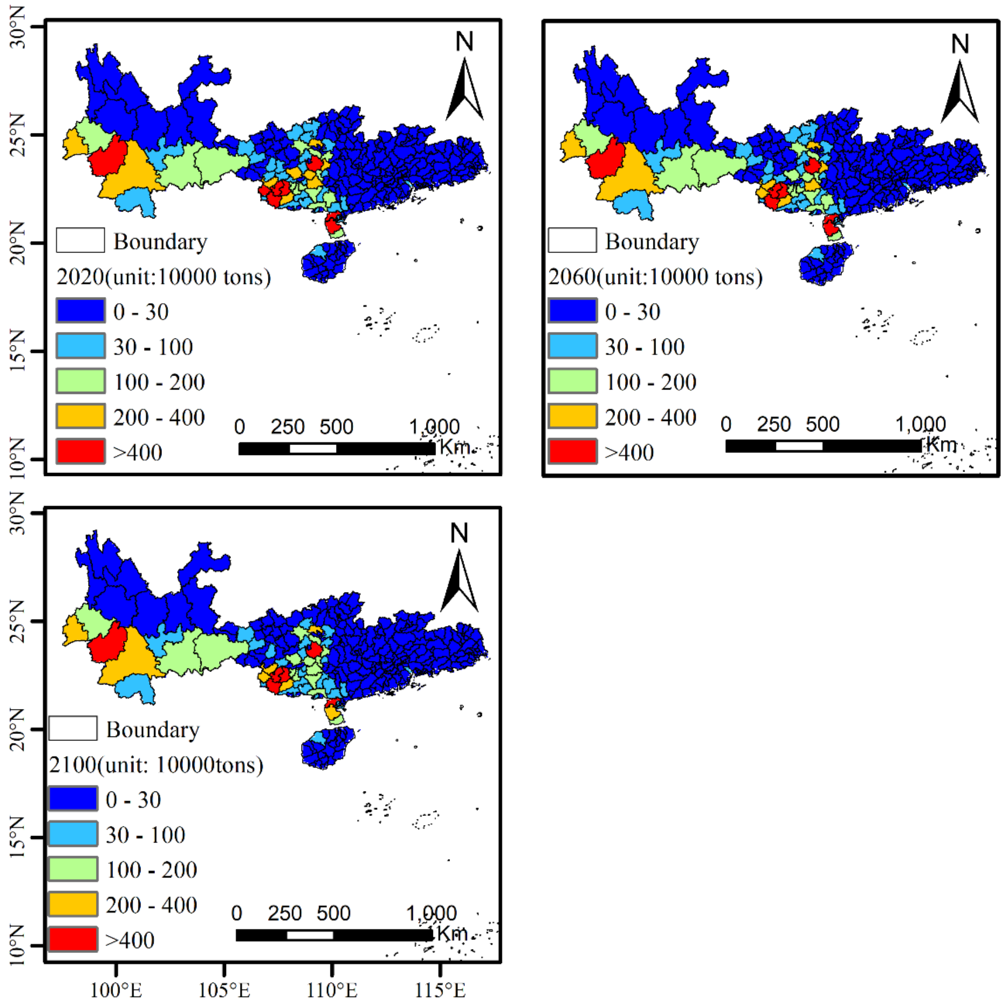

FIG. 9. Distributions of sugarcane yields under SSP370 scenario in (a) 2020, (b) 2060 and (c) 2100.

4. Discussion

Based on the relative soil moisture data from the CLDAS, this study determines the water requirement indicators for sugarcane growth, realizes dynamic monitoring of the daily growth and conducts sugarcane yield forecasts and trend analysis under future scenarios by CMIP6 models.

In this study, the sugarcane adaptable indicators is mainly based on relative soil moisture. As indicated earlier, the relative soil moisture is essential for sugarcane growth. At the early stage of sugarcane growth, the water requirement is relatively low—excessively more water can cause the root rot and death of seedlings, while excessively less water will inhibit the sugarcane growth. In the middle stage of growth, the soil moisture affects the growth and thickening of sugarcane as the water requirement is high—excessively more water can cause the sugarcane leaves to turn yellow, worse growth, rotten roots and even death, while excessively little water will slow down the sugarcane elongation rate (Guozhang 1993), and even more, the stems and leaves may dry out to death. In the later stage of sugarcane growth, the water requirement is relatively low, and soil moisture affects the sugar accumulation. Excessively less water can slow down the sugar accumulation rate, while excessively more water can lead to sugarcane re-growth.

However, there are many other factors affecting the sugarcane growth, such as high temperature, low temperature and other extreme weather disasters (Verma et al. 2019). If these refined data can be obtained, a composite indicators influencing the sugarcane growth can be proposed, and thus the monitoring and analysis of sugarcane growth will be more accurate. In addition, the training data acquired at two levels (municipal and county levels) in constructing the sugarcane yield model are not fine enough, where the data from Yunnan is only at the municipal level, and the data for Guangxi, Guangdong and Hainan are at the county level. In the following work, we should collect more refined yield data, which plays a vital role in yield retrieval by remote sensing data. For example, we can collect yield data on specific sugarcane-producing regions through field surveys.

Combined with weather forecast services, the sugarcane water requirement evaluation based on the CLDAS data conducted in this study can provide daily water requirement of sugarcane planting fields in the next few days for farmers and sugarcane planting companies, aiming to timely supplement soil water for sugarcane growth.

Transition from Regional Competition (SSP3) to Traditional Fossil Fuel Combustion (SSP5), we will find that with the increase of shared socio-economic path (SSPs) scenarios, sugarcane yield under SSP3 socio-economic scenario decreased, and sugarcane yield under SSP5 socio-economic scenario increased between 2022 and 2033. However, after 2050, the decline trend of sugarcane yield under the SSP5 socio-economic scenario model was larger than that under the SSP3 socio-economic scenario model. Therefor, a country's strategy may have major impact on future sugarcane production. The main reasons are that under three future scenarios, air temperature and soil temperature continue to rise, and thus the relative soil moisture continues to decrease. Such meteorological conditions are not adaptable for sugarcane growth. Some effective measures that can be taken to improve the declining trend of sugarcane yield include cultivating new sugarcane varieties with higher yields, improving the ability to cope with climate change and prevent meteorological disasters, promoting the transformation of sugarcane planting from farmer-based to farm-based, and upgrading the modernization level of farming and field management techniques.

5. Conclusions

In this study, we use the CLDAS data to dynamically evaluate the sugarcane water requirement at different growth stages and forecast the sugarcane yields from 2020 to 2100 under three future scenarios. The results suggest that the relative soil moisture from the CLDAS dataset can effectively characterize the growth status of sugarcane and directly affect the final yield.

1) Sugarcane requires more water during the tillering and elongation stages, while less water at seedling-germination and ripening stages.
2) Relative soil moisture has a more significant impact on sugarcane yield during the tillering and elongation stages than during the seedling and ripening stages.
3) Under three future scenarios, sugarcane yield shows an overall decreasing trend during 2020–2100. The sugarcane yield decreases more obviously under the higher emission scenario of SSP585 compared with SSP370.

The evaluation of sugarcane growth adaptability in this study is mainly based on relative soil moisture. In the following work, composite meteorological and environmental indicators will be applied to investigate their adaptabilities for sugarcane growth, aiming to evaluate the sugarcane growth at different stages in a more comprehensive and fine way.

Funding Supported by The National Natural Science Foundation of China Project

(41805049) and Postgraduate Research & Practice Innovation Program of Jiangsu Province (KYCX21_0979).

Author contributions HD, QL, and XZ: contribute research ideas. HD conducted the data analysis and prepared the figures. HD, XZ wrote the first draft of the manuscript. All authors contributed to manuscript revision, read, and approved the submitted version.

Data availability The raw data supporting the conclusions of this article will be made available by the authors, without undue reservation.

Acknowledgements We thank Nanjing Hurricane Translation for reviewing the English language quality of this paper.

Declarations

Ethics approval and consent to participate This research meets all the ethical guidelines, including adherence to the legal requirements of my country. The authors voluntarily agree to participate in this research study.

Consent for publication The authors confirm no conflict of interest and agree with submission of the manuscript to your journal.

Conflict of interest The authors declare no competing interests.

Reference

Aguiar DA, Rudorff BFT, Silva WF, Adami M, Mello MP (2011) Remote Sensing Images in Support of Environmental Protocol: Monitoring the Sugarcane Harvest in São Paulo State, Brazil. REMOTE SENS-BASEL 3:2682-2703 http://doi.org/10.3390/rs3122682

Almeida TIR, De Souza Filho CR, Rossetto R (2006) ASTER and Landsat ETM+ images applied to sugarcane yield forecast. INT J REMOTE SENS 27:4057-4069 http://doi.org/10.1080/01431160600857451

Boucher O, Servonnat J, Albright AL, Aumont O, Balkanski Y, Bastrikov V, Bekki S, Bonnet R, Bony S, Bopp L, Braconnot P, Brockmann P, Cadule P, Caubel A, Cheruy F, Codron F, Cozic A, Cugnet D, D'Andrea F, Davini P, Lavergne C, Denvil S, Deshayes J, Devilliers M, Ducharne A, Dufresne JL, Dupont E, Éthé C, Fairhead L, Falletti L, Flavoni S, Foujols MA, Gardoll S, Gastineau G, Ghattas J, Grandpeix JY, Guenet B, Guez LE, Guilyardi E, Guimberteau M, Hauglustaine D, Hourdin F, Idelkadi A, Joussaume S, Kageyama M, Khodri M, Krinner G, Lebas N, Levavasseur G, Lévy C, Li L, Lott F, Lurton T, Luyssaert S, Madec G, Madeleine JB, Maignan F, Marchand M, Marti O, Mellul L, Meurdesoif Y, Mignot J, Musat I, Ottlé C, Peylin P, Planton Y, Polcher J, Rio C, Rochetin N, Rousset C, Sepulchre P, Sima A, Swingedouw D, Thiéblemont R, Traore AK, Vancoppenolle M, Vial J, Vialard J, Viovy N, Vuichard N (2020) Presentation and Evaluation of the IPSL - CM6A - LR Climate Model. J ADV MODEL EARTH SY 12http://doi.org/10.1029/2019MS002010

Breiman L (2001) Random forests. MACH LEARN 45:5-32

Chen Y, Yuan H (2020) Evaluation of nine sub-daily soil moisture model products over China using high-resolution in situ observations. J HYDROL 588:125054 http://doi.org/10.1016/j.jhydrol.2020.125054

Christofoletti CA, Escher JP, Correia JE, Marinho JFU, Fontanetti CS (2013) Sugarcane vinasse: Environmental implications of its use. WASTE MANAGE 33:2752-2761 http://doi.org/10.1016/j.wasman.2013.09.005

Dong C, Menzel L (2016) Producing cloud-free MODIS snow cover products with conditional probability interpolation and meteorological data. REMOTE SENS ENVIRON 186:439-451 http://doi.org/10.1016/j.rse.2016.09.019

Fang B, Kansara P, Dandridge C, Lakshmi V (2021) Drought monitoring using high spatial resolution soil moisture data over Australia in 2015–2019. J HYDROL 594:125960 http://doi.org/10.1016/j.jhydrol.2021.125960

Fernandes JL, Ebecken NFF, Esquerdo JCDM (2017) Sugarcane yield prediction in

Brazil using NDVI time series and neural networks ensemble. INT J REMOTE SENS 38:4631-4644 http://doi.org/10.1080/01431161.2017.1325531

Foga S, Scaramuzza PL, Guo S, Zhu Z, Dilley RD, Beckmann T, Schmidt GL, Dwyer JL, Joseph Hughes M, Laue B (2017) Cloud detection algorithm comparison and validation for operational Landsat data products. REMOTE SENS ENVIRON 194:379-390 http://doi.org/10.1016/j.rse.2017.03.026

Gao J (2021) Bias-variance decomposition of absolute errors for diagnosing regression models of continuous data. Patterns 2:100309 http://doi.org/10.1016/j.patter.2021.100309

Gocic M, Trajkovic S (2013) Analysis of changes in meteorological variables using Mann-Kendall and Sen's slope estimator statistical tests in Serbia. GLOBAL PLANET CHANGE 100:172-182 http://doi.org/10.1016/j.gloplacha.2012.10.014

Guga S, Xu J, Riao D, Li K, Han A, Zhang J (2021) Combining MaxEnt model and landscape pattern theory for analyzing interdecadal variation of sugarcane climate suitability in Guangxi, China. ECOL INDIC 131:108152 http://doi.org/10.1016/j.ecolind.2021.108152

Guozhang L (1993) Water requirement and irrigation of sugarcane in Guangxi. Guangxi water conservancy and hydropower:62-67 (in Chinese)

Han S, Liu B, Shi C, Liu Y, Qiu M, Sun S (2020) Evaluation of CLDAS and GLDAS Datasets for Near-Surface Air Temperature over Major Land Areas of China. SUSTAINABILITY-BASEL 12:4311 http://doi.org/10.3390/su12104311

Jaiswal D, De Souza AP, Larsen S, LeBauer DS, Miguez FE, Sparovek G, Bollero G, Buckeridge MS, Long SP (2017) Brazilian sugarcane ethanol as an expandable green alternative to crude oil use. NAT CLIM CHANGE 7:788-792 http://doi.org/10.1038/nclimate3410

Kelley M, Schmidt GA, Nazarenko LS, Bauer SE, Ruedy R, Russell GL, Ackerman AS, Aleinov I, Bauer M, Bleck R, Canuto V, Cesana G, Cheng Y, Clune TL, Cook BI, Cruz CA, Del GA, Elsaesser GS, Faluvegi G, Kiang NY, Kim D, Lacis AA, Leboissetier A, LeGrande AN, Lo KK, Marshall J, Matthews EE, McDermid S, Mezuman K, Miller RL, Murray LT, Oinas V, Orbe C, Garcia-Pando CP, Perlwitz

JP, Puma MJ, Rind D, Romanou A, Shindell DT, Sun S, Tausnev N, Tsigaridis K, Tselioudis G, Weng E, Wu J, Yao MS (2020) GISS-E2.1: Configurations and Climatology. J Adv Model Earth Syst 12:e2019M-e2025M http://doi.org/10.1029/2019MS002025

Li Y, Yang L (2015) Sugarcane Agriculture and Sugar Industry in China. SUGAR TECH 17:1-8 http://doi.org/10.1007/s12355-014-0342-1

Long D, Bai L, Yan L, Zhang C, Yang W, Lei H, Quan J, Meng X, Shi C (2019) Generation of spatially complete and daily continuous surface soil moisture of high spatial resolution. REMOTE SENS ENVIRON 233:111364 http://doi.org/10.1016/j.rse.2019.111364

Mohammadi K, Shamshirband S, Tong CW, Arif M, Petković D, Ch S (2015) A new hybrid support vector machine–wavelet transform approach for estimation of horizontal global solar radiation. ENERG CONVERS MANAGE 92:162-171 http://doi.org/10.1016/j.enconman.2014.12.050

Mokhtari A, Noory H, Vazifedoust M (2018) Improving crop yield estimation by assimilating LAI and inputting satellite-based surface incoming solar radiation into SWAP model. AGR FOREST METEOROL 250-251:159-170 http://doi.org/10.1016/j.agrformet.2017.12.250

Nazarenko LS, Tausnev N, Russell GL, Rind D, Miller RL, Schmidt GA, Bauer SE, Kelley M, Ruedy R, Ackerman AS, Aleinov I, Bauer M, Bleck R, Canuto V, Cesana G, Cheng Y, Clune TL, Cook BI, Cruz CA, Genio AD, Elsaesser GS, Faluvegi G, Kiang NY, Kim D, Lacis AA, Leboissetier A, LeGrande AN, Lo KK, Marshall J, Matthews EE, McDermid S, Mezuman K, Murray LT, Oinas V, Orbe C, García Pando CP, Perlwitz JP, Puma MJ, Romanou A, Shindell DT, Sun S, Tsigaridis K, Tselioudis G, Weng E, Wu J, Yao MS (2022) Future Climate Change under SSP Emission Scenarios with GISS‐E2.1. J ADV MODEL EARTH SYhttp://doi.org/10.1029/2021MS002871

O Neill BC, Kriegler E, Ebi KL, Kemp-Benedict E, Riahi K, Rothman DS, van Ruijven BJ, van Vuuren DP, Birkmann J, Kok K, Levy M, Solecki W (2017) The roads ahead: Narratives for shared socioeconomic pathways describing world futures in the 21st century. Global Environmental Change 42:169-180 http://doi.org/10.1016/j.gloenvcha.2015.01.004

O'Neill BC, Tebaldi C, van Vuuren DP, Eyring V, Friedlingstein P, Hurtt G, Knutti R, Kriegler E, Lamarque J, Lowe J, Meehl GA, Moss R, Riahi K, Sanderson BM (2016) The Scenario Model Intercomparison Project (ScenarioMIP) for CMIP6. GEOSCI MODEL DEV 9:3461-3482 http://doi.org/10.5194/gmd-9-3461-2016

Popp A, Calvin K, Fujimori S, Havlik P, Humpenöder F, Stehfest E, Bodirsky BL, Dietrich JP, Doelmann JC, Gusti M, Hasegawa T, Kyle P, Obersteiner M, Tabeau A, Takahashi K, Valin H, Waldhoff S, Weindl I, Wise M, Kriegler E, Lotze-Campen H, Fricko O, Riahi K, Vuuren DPV (2017) Land-use futures in the shared socio-economic pathways. Global Environmental Change 42:331-345 http://doi.org/10.1016/j.gloenvcha.2016.10.002

Pu Y, Liu H, Yan R, Yang H, Xia K, Li Y, Dong L, Li L, Wang H, Nie Y, Song M, Xie J, Zhao S, Chen K, Wang B, Li J, Zuo L (2020) CAS FGOALS-g3 Model Datasets for the CMIP6 Scenario Model Intercomparison Project (ScenarioMIP). ADV ATMOS SCI 37:1081-1092 http://doi.org/10.1007/s00376-020-2032-0

Rajković D, Marjanović Jeromela A, Pezo L, Lončar B, Zanetti F, Monti A, Kondić Špika A (2022) Yield and Quality Prediction of Winter Rapeseed—Artificial Neural Network and Random Forest Models. Agronomy 12:58 http://doi.org/10.3390/agronomy12010058

Rampazo NAM, Picoli MCA, De Castro Teixeira AH, Cavaliero CKN (2021) Water Consumption Modeling by Coupling MODIS Images and Agrometeorological Data for Sugarcane Crops. SUGAR TECH 23:524-535 http://doi.org/10.1007/s12355-020-00919-7

Rongsheng W, Ruifen W, Linxue J, Huizhen W, Kun Y, Haiqing S, Hongjin L, Fengjie Z (2020) CLDAS-based refined agricultural climatic division of spring wheat in Inner Mongolia. Chinese Journal of Ecology 39:2436-2445 (in Chinese)

Rongsheng W, Yunpeng L, Ruifen W, Fengjie Z, Yue S (2021) Refined Climatic

Suitability Division of Sunflower Following Spring Wheat Harvest in Inner Mongolia Based on CLDAS Data. Journal of Arid Meteorology 39:807-815 (in Chinese)

Saeed M, Maqbool A, Ashraf MA, Arshad M, Mehmood K, Usman M, Farid MA (2022) Competency of groundwater recharge of irrigated cotton field subjacent to sowing methods, plastic mulch, water productivity, and yield under climate change. ENVIRON SCI POLLUT R 29:17757-17771 http://doi.org/10.1007/s11356-021-17017-0

Sospedra-Alfonso R, Merryfield WJ, Boer GJ, Kharin VV, Lee W, Seiler C, Christian JR (2021) Decadal climate predictions with the Canadian Earth System Model version 5 (CanESM5). GEOSCI MODEL DEV 14:6863-6891 http://doi.org/10.5194/gmd-14-6863-2021

Sun S, Shi C, Pan Y, Bai L, Xu B, Zhang T, Han S, Jiang L (2020) Applicability Assessment of the 1998–2018 CLDAS Multi-Source Precipitation Fusion Dataset over China. J METEOROL RES-PRC 34:879-892 http://doi.org/10.1007/s13351-020-9101-2

Suon S, Li Y, Porn L, Javed T (2019) Spatiotemporal Analysis of Soil Moisture Drought over China during 2008-2016. Journal of Water Resource and Protection 11:700-712 http://doi.org/10.4236/jwarp.2019.116041

Verma AK, Garg PK, Hari Prasad KS, Dadhwal VK, Dubey SK, Kumar A (2021) Sugarcane Yield Forecasting Model Based on Weather Parameters. SUGAR TECH 23:158-166 http://doi.org/10.1007/s12355-020-00900-4

Verma RR, Srivastava TK, Singh P (2019) Climate change impacts on rainfall and temperature in sugarcane growing Upper Gangetic Plains of India. THEOR APPL CLIMATOL 135:279-292 http://doi.org/10.1007/s00704-018-2378-8

Wang J (2020) Determining the most accurate program for the Mann-Kendall method in detecting climate mutation. THEOR APPL CLIMATOL 142:847-854 http://doi.org/10.1007/s00704-020-03333-x

Wang J, Yu Y (2021) Comprehensive drought monitoring in Yunnan Province, China using multisource remote sensing data. J MT SCI-ENGL 18:1537-1549 http://doi.org/10.1007/s11629-020-6333-7

Wang M, Liu Z, Ali Baig MH, Wang Y, Li Y, Chen Y (2019) Mapping sugarcane in complex landscapes by integrating multi-temporal Sentinel-2 images and machine learning algorithms. LAND USE POLICY 88:104190 http://doi.org/10.1016/j.landusepol.2019.104190

Wang Z, Liu L, Deng Y, Li Y, Zhang G, Lin S, He T (2017) Establishing a Forecast Mathematical Model of Sugarcane Yield and Brix Reduction Based on the Extent of Pokkah Boeng Disease. SUGAR TECH 19:656-661 http://doi.org/10.1007/s12355-017-0538-2

Wei F (2007) Modern climate statistical diagnosis and prediction technology, the second edition edn. Meteorological Press, Beijing (in Chinese)

Wessel B, Huber M, Wohlfart C, Marschalk U, Kosmann D, Roth A (2018) Accuracy assessment of the global TanDEM-X Digital Elevation Model with GPS data. ISPRS J PHOTOGRAMM 139:171-182 http://doi.org/10.1016/j.isprsjprs.2018.02.017

Xia Y, Ek MB, Peters-Lidard CD, Mocko D, Svoboda M, Sheffield J, Wood EF (2014) Application of USDM statistics in NLDAS-2: Optimal blended NLDAS drought index over the continental United States. Journal of Geophysical Research: Atmospheres 119:2947-2965 http://doi.org/10.1002/2013JD020994

Xie Z, Hu Z, Gu L, Sun G, Du Y, Yan X (2017) Meteorological Forcing Datasets for Blowing Snow Modeling on the Tibetan Plateau: Evaluation and Intercomparison. J HYDROMETEOROL 18:2761-2780 http://doi.org/10.1175/JHM-D-17-0075.1

Xu Y, Chen Z, Huang Z, Jiang H, Deng Z, Zhang M (2020) Field Evaluation of New Promising Sugarcane Cultivars for Cold Tolerance in Guangxi, China. SUGAR TECH 22:1007-1017 http://doi.org/10.1007/s12355-020-00853-8

Yu H, Li L, Zhu W, Piao D, Cui G, Kim M, Jeon SW, Lee W (2019) Drought monitoring of the wetland in the Tumen River Basin between 1991 and 2016 using Landsat TM/ETM. INT J REMOTE SENS 40:1445-1459 http://doi.org/10.1080/01431161.2018.1524604

Yuan W, Hu X (2021) Comparison of Heavy Rainfall Events Originated from Different Directions of Beijing City. J METEOROL RES-PRC 34:1299-1308 http://doi.org/10.1007/s13351-020-0051-5

Yue S, Wang C (2004) The Mann-Kendall Test Modified by Effective Sample Size to Detect Trend in Serially Correlated Hydrological Series. WATER RESOUR MANAG 18:201-218 http://doi.org/10.1023/B:WARM.0000043140.61082.60

Yue S, Wang CY (2002) Applicability of prewhitening to eliminate the influence of serial correlation on the Mann-Kendall test. WATER RESOUR RES 38:1-4 http://doi.org/10.1029/2001WR000861

Zhao S, Yu Y, Lin P, Liu H, He B, Bao Q, Guo Y, Hua L, Chen K, Wang X (2020) Datasets for the CMIP6 Scenario Model Intercomparison Project (ScenarioMIP) Simulations with the Coupled Model CAS FGOALS-f3-L. ADV ATMOS SCI 38:329-339 http://doi.org/10.1007/s00376-020-0112-9

Zhaomin K (2019) Sugarcane meteorological intelligent monitoring and intelligent services. Meteorological Press, Beijing (in Chinese)

Zhu X, Hou C, Xu K, Liu Y (2020) Establishment of agricultural drought loss models: A comparison of statistical methods. ECOL INDIC 112:106084 http://doi.org/10.1016/j.ecolind.2020.106084

Zu Q, Mi C, Liu DL, He L, Kuang Z, Fang Q, Ramp D, Li L, Wang B, Chen Y, Li J, Jin N, Yu Q (2018) Spatio-temporal distribution of sugarcane potential yields and yield gaps in Southern China. EUR J AGRON 92:72-83 http://doi.org/10.1016/j.eja.2017.10.005